

[DOI]10.12016/j.issn.2096-1456.202440303

· 临床研究 ·

锥形束CT不同扫描参数对下颌骨骨微结构显示的影响

董琦, 冯永静, 高安天, 林梓桐

南京大学医学院附属口腔医院口腔颌面医学影像科, 南京市口腔医院, 南京大学口腔医学研究所, 江苏南京(210008)

【摘要】 目的 比较锥形束CT(cone beam CT, CBCT)不同扫描参数对下颌骨颏孔前区域骨微结构显示的影响,为合理选择CBCT扫描参数提供基础。方法 获得南京大学医学院附属口腔医院伦理委员会批准,离体研究使用CBCT对8个干燥人下颌骨离体标本进行ProMax 3D Mid扫描,采用5组方案进行扫描,分别为组A:90 kV/6.3 mA,组B:90 kV/8.0 mA,组C:90 kV/10.0 mA,组D:75 kV/8.0 mA,组E:60 kV/8.0 mA,扫描共得到40个CBCT图像;并记录不同扫描条件下的体表入射剂量(entrance surface dose, ESD)及CT剂量指数(computed tomography dose index, CTDI)。将收集的原始CBCT图像导入图像分析软件(Hiscan Analyzer)测量下颌骨兴趣区的4个骨微结构测量参数,分别是骨小梁厚度(trabecular thickness, Tb.Th),骨小梁数目(trabecular number, Tb.N),骨小梁间隙(trabecular space, Tb.Sp),骨小梁体积百分数(bone volume/tissue volume, BV/TV)。回顾性收集临床种植患者分别使用90 kV/6.3 mA、90 kV/8.0 mA、90 kV/10.0 mA中任一组扫描条件得到的CBCT图像共计108个,同样测量下颌骨兴趣区的上述4个参数。使用SPSS 26.0分别比较离体标本及临床患者CBCT图像的4个骨微结构测量参数的差异。结果 离体标本研究结果显示,球管电压及球管电流减低均会导致ESD及CTDI剂量指数下降。当球管电压保持90 kV,球管电流改变时:BV/TV、Tb.N、Tb.Th数值随球管电流增大而增大;Tb.Sp数值随球管电流增大而减小,但4个骨形态参数均无统计学差异($P > 0.05$)。当球管电流保持8.0 mA,球管电压改变时:BV/TV、Tb.N随球管电压增大而减小,Tb.Sp数值随球管电压增大而增大,且BV/TV、Tb.N、Tb.Sp具有统计学差异($P < 0.05$)。临床患者CBCT扫描时,当球管电压为90 kV,而球管电流不同时(6.3、8.0、10.0 mA),4个骨形态参数均不具有统计学差异($P > 0.05$)。结论 本研究中,球管电压固定为90 kV、球管电流增大时下颌骨前区骨微结构显示无差异,临床患者CBCT扫描需显示下颌骨前区骨微结构时可适当减少球管电流以降低患者所受辐射剂量,推荐使用参数90 kV,6.3 mA。

【关键词】 锥形束CT; 球管电压; 球管电流; 骨微结构; 骨形态测量参数; 骨小梁厚度; 骨小梁数目; 骨小梁间隙; 骨小梁体积百分数

【中图分类号】 R78 **【文献标志码】** A **【文章编号】** 2096-1456(2024)12-0945-09

【引用著录格式】 董琦,冯永静,高安天,等.锥形束CT不同扫描参数对下颌骨骨微结构显示的影响[J].口腔疾病防治,2024,32(12):945-953. doi:10.12016/j.issn.2096-1456.202440303.

Effects of different scanning parameters of cone beam CT on displaying microstructure of mandible DONG

Qi, FENG Yongjing, GAO Antian, LIN Zitong. Department of Dentomaxillofacial Radiology, Nanjing Stomatological Hospital, Affiliated Hospital of Medical School, Institute of Stomatology, Nanjing University, Nanjing 210008, China

Corresponding author: LIN Zitong, Email: linzitong710@163.com, Tel: 86-25-83620350

【Abstract】 Objective To compare the effect of different scanning parameters of cone beam computed tomography (CBCT) on displaying trabecular microstructure in the anterior region of the mental foramen of the mandible, and to pro-



微信公众号

【收稿日期】2024-08-19; **【修回日期】**2024-11-24

【基金项目】国家自然科学基金青年基金项目(82201135)

【作者简介】董琦,住院医师,硕士在读,Email:3115385356@qq.com

【通信作者】林梓桐,主任医师,博士,Email:linzitong710@163.com, Tel:86-25-83620350

vide a basis for the rational selection of CBCT scanning parameters. **Methods** This study was approved by the Ethics Committee of the Affiliated Stomatological Hospital, Medical School of Nanjing University. An in vitro study was conducted using CBCT (ProMax 3D Mid) to scan eight dry human mandibular specimens with five scanning protocols: Group A: 90 kV/6.3 mA, Group B: 90 kV/8.0 mA, Group C: 90 kV/10.0 mA, Group D: 75 kV/8.0 mA, and Group E: 60 kV/8.0 mA, resulting in a total of 40 CBCT images. Entrance surface dose (ESD) and computed tomography dose index (CTDI) under different scanning conditions were recorded. The original CBCT images were imported into the image analysis software (Hiscan Analyzer) to measure four trabecular bone microstructural parameters in the region of interest of the mandible: trabecular thickness (Tb.Th), trabecular number (Tb.N), trabecular space (Tb.Sp), and bone volume/tissue volume (BV/TV). A total of 108 CBCT images were retrospectively collected from clinical implant patients using any of the 90 kV/6.3 mA, 90 kV/8.0 mA, or 90 kV/10.0 mA scanning conditions, and the above four parameters of the region of interest of the mandible were also measured. SPSS 26.0 software was used to compare the differences in the four trabecular bone microstructural parameters between the CBCT images of the mandibular specimens in vitro and clinical patients in vivo. **Results** The in vitro study results showed that reducing the tube voltage and tube current would lead to a decrease in the ESD and CTDI. When the tube voltage was maintained at 90 kV and the tube current was changed, BV/TV, Tb.N, and Tb.Th values increased with the increase of tube current; Tb.Sp values decreased with the increase of tube current, but there was no statistically significant difference in the four bone morphological parameters ($P > 0.05$). When the tube current was maintained at 8.0 mA and the tube voltage was altered, BV/TV and Tb.N decreased with the increase of tube voltage, Tb.Sp values increased with the increase of tube voltage, and BV/TV, Tb.N, and Tb.Sp showed statistically significant differences ($P < 0.05$). In clinical patients undergoing CBCT scanning, when the tube voltage was 90 kV and the tube current was different (6.3, 8.0, 10.0 mA), there was no statistically significant difference in the four bone morphological parameters ($P > 0.05$). **Conclusions** In this study, when the tube voltage was fixed at 90 kV, there was no difference in the trabecular microstructure of the anterior region of the mandible when the tube current was increased. When CBCT scanning of clinical patients needs to show the trabecular microstructure of the anterior region of the mandible, the tube current can be appropriately reduced to decrease the radiation dose received by the patient. Thus, it is recommended to use the parameters 90 kV and 6.3 mA for CBCT scanning.

【Key words】 cone-beam computed tomography; tube voltage; tube current; trabecular microstructure; trabecular bone microarchitectural parameters; trabecular thickness; trabecular number; trabecular space; bone volume / tissue volume

J Prev Treat Stomatol Dis, 2024, 32(12): 945-953.

【Competing interests】 The authors declare no competing interests.

This study was supported by the grants from National Natural Science Foundation of China (No. 82201135).

锥形束CT(cone beam CT, CBCT)近年来被广泛运用于种植术前骨评价^[1-2]。种植术前骨评价包括骨密度和骨质量的评价。骨微结构在种植术前骨质量和植骨术后骨整合等方面评价中具有重要价值。临床上,由于不同CBCT设备扫描设置的球管电压、球管电流、重建层厚、曝光时间等均存在一定差异,可导致同一患者不同CBCT设备图像显示的骨微结构不同^[3],并可能导致骨质量评估结果的差异。另一方面,不同的球管电压、球管电流、曝光时间等扫描参数下患者受到的辐射剂量也不同^[4]。如何保证骨质量评估的准确性并尽可能降低患者所受辐射剂量,一直以来都是放射类检查中需要重点关注的问题之一。因此,本研究针对不同球管电压和球管电流对CBCT图像骨微结构显示的影响进行离体标本

和临床研究,比较不同扫描条件下的骨微结构定量参数骨小梁数目(trabecular number, Tb.N),骨小梁间隙(trabecular space, Tb.Sp),骨小梁厚度(trabecular thickness, Tb.Th),骨小梁体积百分数(bone volume / tissue volume, BV/TV)^[5-6]是否存在差异,为临床上合理选择CBCT球管电压和球管电流用于评价种植患者骨微结构提供参考。

1 资料和方法

1.1 研究对象

本研究经过南京大学医学院附属口腔医院伦理委员会的批准(审批号:JX-2023-NL66)。本研究共借用了8个本院解剖教研室无法区分年龄、性别的干燥人下颌骨离体标本用于CBCT扫描,CBCT

扫描使用 ProMax 3D Mid (Planmeca, 芬兰)。扫描时,将下颌骨标本的双侧下颌骨下缘平放在扫描平台的中心区域上进行扫描。曝光时,记录不同球管电压及球管电流扫描时的体表入射剂量 (entrance surface dose, ESD) 及 CT 剂量指数 (com-

puted tomography dose index, CTDI)(表1)。有效曝光时间:13.5 s, 扫描重建层厚为 0.4 mm, 视野:16 cm×10 cm。本研究对下颌骨标本共使用了5个扫描方案进行重复扫描(表1及图1),共获取40个 CBCT 数据。

表1 离体下颌骨标本的CBCT扫描参数

Table 1 CBCT scanning parameters of mandible specimens *in vitro*

Scanning protocol	Tube voltage/kV	Tube current/mA	ESD/(mGy·cm ²)	CTDI/mGy
A	90	6.3	706	3.2
B	90	8.0	891	4.1
C	90	10.0	1 123	5.13
D	75	8.0	467	1.8
E	60	8.0	181	0.6

ESD: entrance surface dose; CTDI: computed tomography dose index

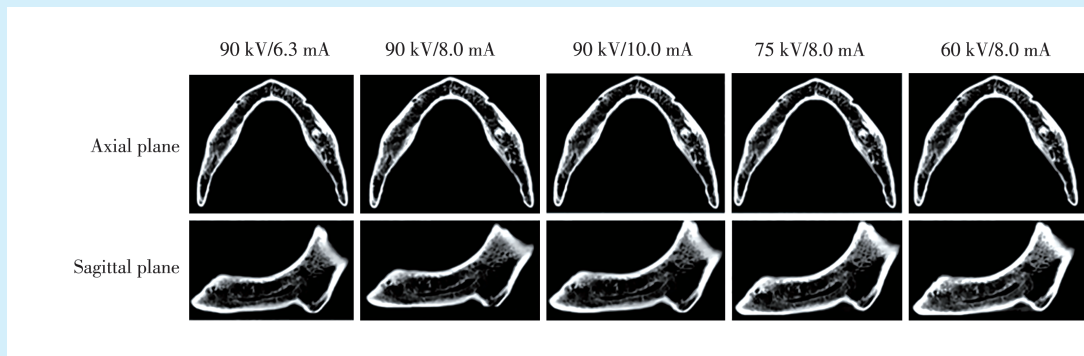


Figure 1 CBCT axial and sagittal images of the same mandibular specimen under different tube voltage and tube current combinations

图1 同一离体下颌骨标本在不同球管电压及球管电流组合下的CBCT轴位及矢状位图像

使用PASS2021软件(v21.0.3)进行临床研究样本量估计,以预实验的样本均数±标准差(1.01±0.14)、(1.34±0.40)、(1.38±0.52)作为估计值,检验水准取0.05,检验效能取0.8,通过预实验估算每组样本量33。

临床CBCT图像纳入标准:①牙列缺损的种植患者;②无大面积颌骨缺损;③患者CBCT扫描使用球管电压为90 kV,球管电流为6.3 mA或8.0 mA或10.0 mA(图2);④CBCT图像清晰,无运动伪影。

排除标准:①种植术后患者;②重度牙周炎患者;③正畸、正颌治疗史;④颌面部肿瘤患者;⑤颌面部外伤史;⑥严重基础疾病患者;⑦全身系统疾病伴发颌骨改变患者。临床研究采用回顾性队列研究,回顾收集2024年1月至2024年7月本院种植科患者因诊疗需要拍摄的CBCT图像。本研究最终共纳入种植患者CBCT数据108例,球管电压为90 kV,球管电流为6.3 mA、8.0 mA、10.0 mA各

36例,患者年龄18~35岁,每组男女各18例。

1.2 图像处理及分析

所有CBCT图像以DICOM格式导入软件Hiscan Analyzer。旋转CBCT容积数据,使得双侧颞孔区结构对称,并在连续的CBCT轴位图像上寻找到颞孔与颊侧皮质骨相交的最大径层面(S0),并以此层图像为中心,向上、下各取3个层面(S-3~S3),一共7个层面,在该7个层面上勾画兴趣区(region of interest, ROI)。ROI的近远中边界在S0上确定并勾画(图3),且S0层面上的近远中边界保留在S-3~S3上使用,所有7个层面上的颊舌侧边界取颊舌侧骨皮质,7层图像的ROI共同构成测量容积(volume of interest, VOI),设定二值化阈值并对VOI进行二值化处理,经分析计算,得到骨小梁数目(trabecular number, Tb.N),骨小梁间隙(trabecular space, Tb.Sp),骨小梁厚度(trabecular thickness, Tb.Th),骨小梁体积百分数(bone volume / tissue volume, BV/TV)。具体流程见图4。

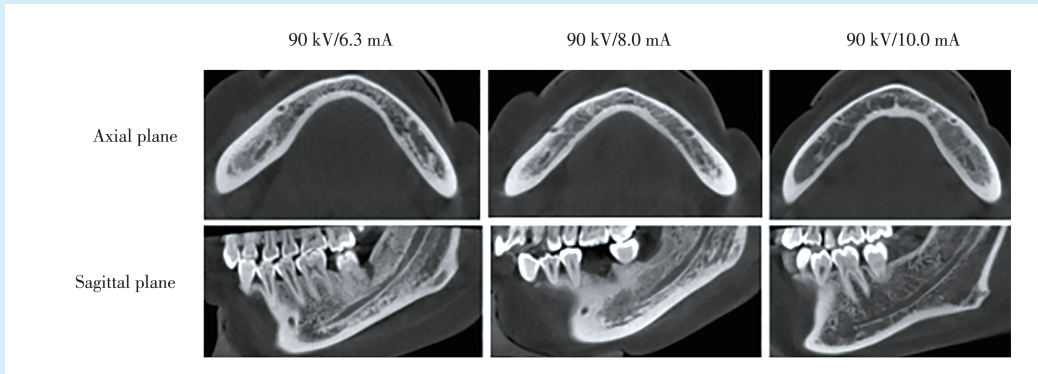
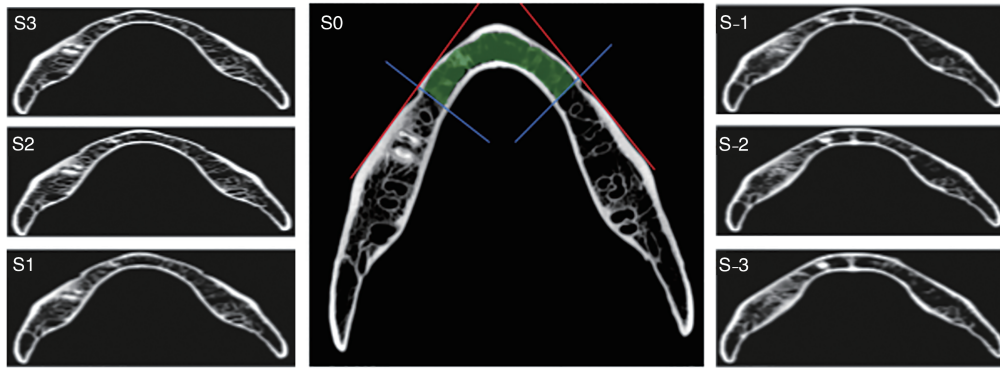


Figure 2 CBCT axial and sagittal images of clinical patients under the same tube voltage and different tube currents
图2 临床患者同一球管电压不同球管电流下的CBCT轴位及矢状位图像



S0 denotes the plane where the mental foramen intersects with the buccal cortical bone with maximum diameter, S1-S3 denote three upward planes of S0, and S-1-S-3 denote three downward planes of S0. Region of interest (ROI) on S0: a tangent line (red) is drawn along the edge of the buccal cortical bone in the mental foramen area, and a perpendicular line (blue) is drawn passing through the anterior edge of the mental foramen. The blue lines on the left and right sides are the distal boundaries, and the cortical bone on the buccal and lingual sides is the buccal lingual boundary

Figure 3 Localization of the region of interest on the mandible
图3 下颌骨兴趣区层面的定位

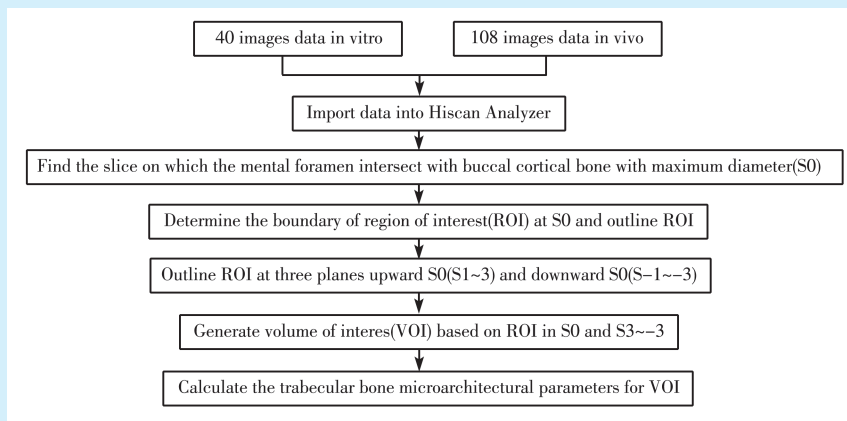


Figure 4 Flow chart of calculating trabecular bone microarchitectural parameters
图4 骨微结构参数计算流程

1.3 统计学方法

使用SPSS26.0软件对离体数据进行统计学分析。由于离体标本研究的计量资料样本量小、未满足正态性及方差齐性,在多组间采取Friedman-*M*检验多重比较采取Bonferroni法对检验水准进行校正,检验水准取双侧0.05,统计数值用中位数(四分位间距)表示。单因素方差分析比较患者年龄,卡方检验分析性别分布,各组间的年龄、性别无统计学差异。采用单因素方差分析进行单独效应分析,组内多重比较使用LSD法,检验水准取双侧0.05,统计数值用平均值±标准差表示。

2 结果

离体标本研究中:当球管电压固定为90 kV, BV/TV、Tb.N、Tb.Th随球管电流增大而增大;Tb.Sp随球管电流增大而减小,但3种球管电流下的骨微结构参数无统计学差异($P > 0.05$)(表2);当球管电流固定为8.0 mA时, BV/TV、Tb.N随球管电压增大而减小, Tb.Sp随球管电压增大而增大, BV/TV、Tb.N、Tb.Sp骨微结构参数有统计学差异($P < 0.05$)(表3)。

临床研究中:使用固定的90 kV球管电压,球管电流改变时,骨微结构的4个参数均不具有差异($P > 0.05$)(表4)。

表2 球管电压90 kV,不同球管电流下离体下颌骨标本骨微结构测量参数的四分位表

Table 2 Quartile table showing trabecular bone microarchitectural parameters of mandibular specimens under a tube voltage of 90 kV and different tube currents

Tube current/mA	BV/TV	Tb.N	Tb.Sp	Tb.Th
6.3	0.26(0.19-0.45)	0.28(0.25-0.35)	2.64(1.78-3.05)	1.10(0.93-1.28)
8.0	0.28(0.20-0.45)	0.29(0.25-0.34)	2.35(1.70-3.09)	1.12(0.94-1.29)
10.0	0.32(0.19-0.49)	0.29(0.27-0.33)	2.32(1.82-2.77)	1.19(0.90-1.34)
χ^2	0.75	0.75	1.75	0.75
<i>P</i>	0.687	0.687	0.417	0.687

BV/TV: bone volume/tissue volume; Tb.N: trabecular number; Tb.Sp: trabecular space; Tb.Th: trabecular thickness

表3 球管电流8.0 mA时,不同球管电压下离体下颌骨标本骨微结构测量参数的四分位表

Table 3 Quartile table showing trabecular bone microarchitectural parameters of mandibular specimens under a tube current of 8.0 mA and different tube voltages

Tube voltage/kV	BV/TV	Tb.N	Tb.Sp	Tb.Th
60	0.36(0.26-0.59)	0.34(0.28-0.41)	1.92(1.18-2.60)	1.14(1.02-1.28)
75	0.31(0.22-0.56)	0.32(0.28-0.38)	2.09(1.34-2.71)	1.08(0.95-1.27)
90	0.28(0.22-0.50)	0.29(0.25-0.34)	2.35(1.70-3.09)	1.12(0.94-1.29)
χ^2	10.75	13.00	13.00	2.25
<i>P</i>	0.005	0.002	0.002	0.325

BV/TV: bone volume/tissue volume; Tb.N: trabecular number; Tb.Sp: trabecular space; Tb.Th: trabecular thickness

表4 球管电压90 kV时,不同球管电流下临床患者的骨微结构测量参数

Table 4 Trabecular bone microarchitectural parameters of clinical patients under a tube voltage of 90 kV and different tube currents

Tube current/mA	BV/TV	Tb.N	Tb.Sp	Tb.Th
6.3	0.76±0.11	0.32±0.04	1.16±0.26	1.97±0.45
8	0.73±0.14	0.34±0.08	1.21±0.30	1.92±0.56
10	0.71±0.16	0.31±0.03	1.27±0.33	1.98±0.53
<i>F</i>	1.384	1.520	1.134	0.123
<i>P</i>	0.255	0.223	0.326	0.884

BV/TV: bone volume/tissue volume; Tb.N: trabecular number; Tb.Sp: trabecular space; Tb.Th: trabecular thickness

3 讨论

CBCT 目前已被广泛运用于种植术前骨评估^[7-9],种植术前骨评估包括骨密度和骨质量(骨微结构)的评估。但在临床上,不同的CBCT设备使用的扫描方式存在一定的差异,且同一品牌CBCT可以有多种扫描模式^[10-11],如何在临床上针对不同的患者采用恰当的扫描方式,同时客观看待不同CBCT设备显示的骨微结构,从而实现种植术前准确的骨质量评价是本研究的研究目标。基于此,本研究使用ProMax 3D Mid CBCT的不同扫描参数对8个干燥人下颌骨离体标本进行扫描,并进行了骨微结构的定量测量与比较分析,用于探讨CBCT不同扫描球管电压、球管电流对骨微结构显示的差异,同时收集临床上使用ProMax 3D Mid CBCT推荐球管电压、不同球管电流患者的CBCT图像,并比较其显示的骨微结构参数差异,为临床上合理选择球管电压和球管电流提供一定依据。

本研究选取了4个具有代表性的骨形态计量学参数,分别是骨小梁数目(Tb.N)、骨小梁间隙(Tb.Sp)、骨小梁厚度(Tb.Th)、骨小梁体积百分数(BV/TV)。其中,骨小梁厚度(Tb.Th)、骨小梁间隔(Tb.Sp)和骨小梁数量(Tb.N)可以从侧面推断骨小梁网的空间架构;骨小梁体积百分数(BV/TV)可直接反应骨量的变化情况^[5]。这4个指标中,Tb.N、Tb.Th和BV/TV可被认为是骨微结构的正向指标,而Tb.Sp可被看作骨微结构的负向指标,本研究还对CBCT中常用的剂量指数,体表入射剂量(ESD)和CT剂量指数(CTDI)进行测量^[12]。

颌骨骨微结构(颌骨骨小梁形态和微观结构)的评价方法有:破坏检测方法和非破坏检测方法^[13]。破坏检测包括骨活检的二维切片,结合使用体视学方法计算骨形态测量参数进行分析,但因骨活检具有创伤,限制了其临床应用,一般不提倡用于患者的诊断工作中。显微CT(micro-computed tomography, micro-CT)具有无损检测、高分辨成像、微米级测量等优点,是评价颌骨骨微结构的非破坏检测方法,目前被认为是骨微结构检测的金标准^[14]。然而,因为micro-CT过小的视野、过长的扫描时间和过高的辐射剂量,它的使用仅限在小动物模型或人体活检标本评估上,目前并不能用于临床^[15]。CBCT扫描方式与micro-CT类

似,且扫描范围较大、辐射剂量低^[16],目前已经被广泛运用于种植术前骨评价^[17]。2017年Liang等^[18]的研究表明体素125 μm的CBCT评估小梁结构显示出与micro-CT相当的准确性。2017年Van Dessel等^[15]通过使用市面上常见的七台不同的CBCT扫描仪与Micro-CT及多层螺旋CT扫描的图像作对比,其研究结果表明:Micro-CT与CBCT的大多数骨小梁模式相同且骨小梁结构参数之间存在较高的ICC值(ICC >0.70),这提示CBCT在评价骨微结构方面有很强的可行性^[19],可以为种植术前骨评估提供指导。因此,使用CBCT进行骨微结构的评价具有较好的理论基础^[20]。

离体标本研究中,当保持球管电压不变:Tb.N、Tb.Th、BV/TV随球管电流的增大而增大,Tb.Sp随球管电流的增大而减小;这意味着较大的球管电流显示的骨微结构更加丰富^[21],较大球管电流的CBCT图像可显示更加细致的骨微结构,这也与2021年Sarmiento等^[22]的研究结果一致。但本研究中3种球管电流值6.3、8.0、10.0 mA之间的4个骨形态测量参数并不具有统计学差异($P > 0.05$),这也就意味着虽然增大球管电流可提升显示的骨微结构的细节,但是其影响较为有限,综合考虑到增大球管电流会导致患者所受到的辐射剂量增大^[23],因此当CBCT图像用于观察骨微结构时,并不推荐使用过高的球管电流,使用相对较低的球管电流,并不会导致图像质量的明显下降^[24],不会影响种植术前评估^[5]。考虑到临床CBCT扫描时存在颌面部软组织、骨髓等因素的影响,为了验证离体标本研究中球管电流下降不会导致骨微结构显示的统计学差异这一结果是否确切,本研究进一步回顾性收集了临床上不同患者扫描时使用相同球管电压、不同球管电流的CBCT图像,并比较了这些CBCT图像上4个骨微结构测量参数是否存在差异。由于90 kV是临床上使用的较为广泛的CBCT扫描电压,因此临床研究中,扫描方案被设置为固定球管电压(90 kV),不同球管电流(6.3、8.0、10.0 mA)。临床研究结果显示,当球管电压不变、球管电流减小时,患者所受辐射暴露越小且骨微结构显示并不具有统计学差异。当然也应该考虑到,本研究中当球管电压保持不变、

球管电流改变时骨微结构参数的改变并不具有统计学差异,也可能与扫描参数的选择范围不够广泛等因素有关。所以,综合上述研究结果,在临床工作中可以适当降低球管电流,减少患者的辐射暴露剂量,这也与目前国际上所提倡的对种植患者低剂量CBCT扫描的理念一致^[25]。

本研究中,当球管电流固定(8.0 mA),球管电压逐步增高时(60~90 kV),下颌骨标本的BV/TV、Tb.N随球管电压增大而减小,Tb.Sp随球管电压增大而增大,说明随着球管电压的增大,显示的骨微结构变少、变稀疏,且在保持球管电流为8.0 mA时,3种球管电压下的BV/TV、Tb.N、Tb.Sp均具有统计学差异。考虑到增大球管电压会明显增加临床患者所受的辐射剂量^[26-27],理论上,应选择较低的球管电压对患者进行扫描。但是,降低球管电压时,X射线穿透力会明显降低^[28],探测器接收到的X射线量也明显下降,图像质量下降会比降低球管电流更加明显^[29]。且临床情况下,由于颌面部软组织、颌骨含水量、骨髓等因素的影响,过低的球管电压下图像质量会进一步下降,因此目前临床上并不推荐使用低于90 kV的球管电压^[20]。在临床上,应根据患者不同情况选择恰当的扫描剂量。当然,颌骨骨微结构的准确显示不仅对种植患者骨质量评价具有重要意义,对于颌骨肿瘤性病变诊断、骨质疏松诊断、炎症修复评价、骨折愈合评价等均具有重要参考价值。因此,尤其是在疾病纵向对比时要充分考虑到不同扫描条件对骨微结构呈现的影响,从而更加准确地进行疾病诊断和预后分析。

本研究尚有一定不足,首先就是临床数据及离体的下颌骨标本样本量均较小,其次离体的下颌骨标本外部无软组织影响,测量的数值与临床测量存在一定差异^[8],在后续研究中可考虑进行软组织模拟进一步评估软组织对成像质量和骨微结构参数测量的可能影响;再次由于机型的影响,本研究所使用的CBCT机未能将球管电压调至110 kV及120 kV进行评价,而临床上部分CBCT设备使用的球管电压为110 kV或120 kV。此外,还应该充分考虑到CBCT骨微结构评价还会受到扫描算法^[30]、金属伪影^[31]、运动伪影^[32]、空间分辨率限制^[33]、容积效应^[34]、设备性能差异等很多因素影

响,这些因素对于骨微结构显示的影响尚有待进一步研究。

本研究中的离体标本研究显示,球管电压保持90 kV、球管电流增大时,CBCT显示的骨小梁厚度、骨小梁数目、骨小梁体积百分数增大,骨小梁间隙减小,但无统计学差异;当球管电流保持8.0 mA、球管电压增大时,CBCT显示的骨小梁数目、骨小梁体积百分数减少,骨小梁间隙增大,且具有统计学差异。临床研究显示球管电压保持90 kV、不同球管电流下的患者的下颌骨骨微结构显示无明显差异。因此,临床上建议可以适当降低球管电流进行下颌骨前区骨微结构的评估。

【Author contributions】 Dong Q performed the research, and wrote the manuscript. Feng YJ analyzed the data and revised the article. Gao AT provided experimental methods and followed up. Lin ZT gave a comprehensive analysis and guidance to the thesis. All authors read and approved the final manuscript submitted.

参考文献

- [1] Vyas R, Khurana S, Khurana D, et al. Cone beam computed tomography (CBCT) evaluation of alveolar bone thickness and root angulation in anterior maxilla for planning immediate implant placement[J]. *Cureus*, 2023, 15(4): e37875. doi: 10.7759/cureus.37875.
- [2] Song D, Shujaat S, de Faria Vasconcelos K, et al. Diagnostic accuracy of CBCT versus intraoral imaging for assessment of peri-implant bone defects[J]. *BMC Med Imaging*, 2021, 21(1): 23. doi: 10.1186/s12880-021-00557-9.
- [3] Waldthaler A, Reuterwall-Hansson M, Arnelo U, et al. Radiation dose in cone beam CT guided ERCP[J]. *Eur J Radiol*, 2020, 123: 108789. doi: 10.1016/j.ejrad.2019.108789.
- [4] de Castro HS, Kehrwald R, Matheus RA, et al. Influence of low-dose protocols of CBCT on dental implant planning[J]. *Int J Oral Maxillofac Implants*, 2021, 36(2): 307 - 312. doi: 10.11607/jomi.8773.
- [5] 魏占英, 章振林. Micro-CT在骨代谢研究中骨微结构指标的解读及应用价值[J]. *中华骨质疏松和骨矿盐疾病杂志*, 2018, 11(2): 200-205. doi: 10.3969/j.issn.1674-2591.2018.02.016.
Wei ZY, Zhang ZL. Interpretation and application of micro-CT to obtain microstructure index in bone metabolism research[J]. *Chin J Osteoporos Bone Miner Res*, 2018, 11(2): 200-205. doi: 10.3969/j.issn.1674-2591.2018.02.016.
- [6] Tabassum A, Chainchel Singh MK, Ibrahim N, et al. Quantifications of mandibular trabecular bone microstructure using cone beam computed tomography for age estimation: a preliminary study [J]. *Biology(Basel)*, 2022, 11(10): 1521. doi: 10.3390/biology11101521.

- [7] Schulze RKW, Drage NA. Cone-beam computed tomography and its applications in dental and maxillofacial radiology[J]. Clin Radiol, 2020, 75(9): 647-657. doi: 10.1016/j.crad.2020.04.006.
- [8] 丁黔川, 冯红超, 韦敬, 等. 成人下颌前行管的锥形束CT影像学研究[J]. 口腔疾病防治, 2022, 30(3): 200-206. doi: 10.12016/j.issn.2096-1456.2022.03.007.
Ding QC, Feng HC, Wei J, et al. Imaging study of the mandibular forward canal in adults based on cone beam CT[J]. J Prev Treat Stomatol Dis, 2022, 30(3): 200-206. doi: 10.12016/j.issn.2096-1456.2022.03.007.
- [9] 苏镇亚, 李诗琪, 莫安春. 上颌美学区唇侧骨板部分缺损行即刻种植和延期种植的前瞻队列研究[J]. 口腔疾病防治, 2022, 30(7): 483-490. <https://doi.org/10.12016/j.issn.2096-1456.2022.07.004>.
Su ZY, Li SQ, Mo AC. A prospective cohort study of immediate implantation and delayed implantation for a labial bony dehiscence defect in the maxillary aesthetic area[J]. J Prev Treat Stomatol Dis, 2022, 30(7): 483-490. doi: 10.12016/j.issn.2096-1456.2022.07.004.
- [10] Fuglsig JMCES, Reis INRD, Yeung AWK, et al. The current role and future potential of digital diagnostic imaging in implant dentistry: a scoping review[J]. Clin Oral Implants Res, 2024, 35(8): 793-809. doi: 10.1111/clr.14212.
- [11] Kottou S, Zapros A, Stefanopoulou N, et al. Cone beam CT in dental implant planning: how close are patient dosimetry results with data from phantom studies found in literature?[J]. Radiat Prot Dosimetry, 2019, 187(3): 321-326. doi: 10.1093/rpd/ncz169.
- [12] Ohene-Botwe B, Anim-Sampong S, Nkansah J. Development of size-specific dose estimates for common computed tomography examinations: a study in Ghana[J]. J Radiol Prot, 2023, 43(1). doi: 10.1088/1361-6498/acb5aa.
- [13] Van Dessel J, Huang Y, Depyere M, et al. A comparative evaluation of cone beam CT and micro-CT on trabecular bone structures in the human mandible[J]. Dentomaxillofac Radiol, 2013, 42(8): 20130145. doi: 10.1259/dmfr.20130145.
- [14] Burghardt AJ, Link TM, Majumdar S. High-resolution computed tomography for clinical imaging of bone microarchitecture[J]. Clin Orthop Relat Res, 2011, 469(8): 2179-2193. doi: 10.1007/s11999-010-1766-x.
- [15] Van Dessel J, Nicolielo LF, Huang Y, et al. Accuracy and reliability of different cone beam computed tomography (CBCT) devices for structural analysis of alveolar bone in comparison with multislice CT and micro-CT[J]. Eur J Oral Implantol, 2017, 10(1): 95-105.
- [16] Koç A, Eroğlu CN, Bilgili E. Assessment of prevalence and volumetric estimation of possible Stafne bone concavities on cone beam computed tomography images[J]. Oral Radiol, 2020, 36(3): 254-260. doi: 10.1007/s11282-019-00402-4.
- [17] Key YW, Ng ZB, Al-Namnam NM, et al. The location of the mental foramen in relation to the biometrics of the lower dentition and mandibular arch: a cross-sectional study[J]. Ital J Anat Embryol, 2022, 125(1): 103-119. doi: 10.36253/ijae-13035.
- [18] Liang X, Zhang Z, Gu J, et al. Comparison of micro-CT and cone beam CT on the feasibility of assessing trabecular structures in mandibular condyle[J]. Dentomaxillofac Radiol, 2017, 46(5): 20160435. doi: 10.1259/dmfr.20160435.
- [19] Kulah K, Gulsahi A, Kamburoğlu K, et al. Evaluation of maxillary trabecular microstructure as an indicator of implant stability by using 2 cone beam computed tomography systems and micro-computed tomography[J]. Oral Surg Oral Med Oral Pathol Oral Radiol, 2019, 127(3): 247-256. doi: 10.1016/j.oooo.2018.11.014.
- [20] Min CK, Kim KA. Quantitative analysis of metal artefacts of dental implant in CBCT image by correlation analysis to micro-CT: a microstructural study[J]. Dentomaxillofac Radiol, 2021, 50(3): 20200365. doi: 10.1259/dmfr.20200365.
- [21] Ito M, Chida K, Onodera S, et al. Evaluation of radiation dose and image quality for dental cone-beam computed tomography in pediatric patients[J]. J Radiol Prot, 2023, 43(3). doi: 10.1088/1361-6498/acf868.
- [22] Sarmiento VA, de Oliveira Gonzalez TFL, Lopes RT, et al. A comparative study of multidetector computed tomography, cone beam computed tomography, and computed microtomography on trabecular bone structures in the human mandible: an *ex vivo* study[J]. J Comput Assist Tomogr, 2021, 45(4): 552-556. doi: 10.1097/RCT.0000000000001191.
- [23] Yeung AWK, Jacobs R, Bornstein MM. Novel low-dose protocols using cone beam computed tomography in dental medicine: a review focusing on indications, limitations, and future possibilities [J]. Clin Oral Investig, 2019, 23(6): 2573-2581. doi: 10.1007/s00784-019-02907-y.
- [24] Park HN, Min CK, Kim KA, et al. Optimization of exposure parameters and relationship between subjective and technical image quality in cone-beam computed tomography[J]. Imaging Sci Dent, 2019, 49(2): 139-151. doi: 10.5624/isd.2019.49.2.139.
- [25] Kaaber L, Matzen LH, Schropp L, et al. Low-dose CBCT protocols in implant dentistry: a systematic review[J]. Oral Surg Oral Med Oral Pathol Oral Radiol, 2024, 138(3): 427-439. doi: 10.1016/j.oooo.2024.03.013.
- [26] Kim J, Jeon H, Kyung Kim H. Monte carlo dose assessment in dental cone-beam computed tomography[J]. Radiat Prot Dosimetry, 2021, 193(3/4): 190-199. doi: 10.1093/rpd/ncab039.
- [27] Sawicki P, Zawadzki PJ, Regulski P. The impact of cone-beam computed tomography exposure parameters on peri-implant artifacts: a literature review[J]. Cureus, 2022, 14(3): e23035. doi:

- 10.7759/eureus.23035.
- [28] Baumann E, Bornstein MM, Dalstra M, et al. Image quality assessment of three cone beam computed tomography scanners-an analysis of the visibility of anatomical landmarks[J]. *Eur J Orthod*, 2022, 44(5): 513-521. doi: 10.1093/ejo/ejac004.
- [29] 施雄, 李生娇, 周剑萍, 等. 低剂量锥形束CT扫描可行性的实验研究[J]. *华西口腔医学杂志*, 2020, 38(4): 415-418. doi: 10.7518/hxkq.2020.04.011.
- Shi X, Li SJ, Zhou JP, et al. Experimental study on the feasibility of low-dose cone beam computed tomography scanning[J]. *West China J Stomatol*, 2020, 38(4): 415 - 418. doi: 10.7518 / hxkq.2020.04.011.
- [30] McLaughlin V, Liu J, Kalim S, et al. Application of metal artifact reduction algorithm for CBCT diagnosis of temporary anchorage device-tooth root contact: inadequate to reduce false-positive rate [J]. *Dentomaxillofac Radiol*, 2023, 52(6): 20220396. doi: 10.1259/dmfr.20220396.
- [31] Park HS, Seo JK, Hyun CM, et al. A fidelity-embedded learning for metal artifact reduction in dental CBCT[J]. *Med Phys*, 2022, 49(8): 5195-5205. doi: 10.1002/mp.15720.
- [32] Sun T, Jacobs R, Pauwels R, et al. A motion correction approach for oral and maxillofacial cone-beam CT imaging[J]. *Phys Med Biol*, 2021, 66(12). doi: 10.1088/1361-6560/abfa38.
- [33] Ronkainen AP, Al-Gburi A, Liimatainen T, et al. A dose-neutral image quality comparison of different CBCT and CT systems using paranasal sinus imaging protocols and phantoms[J]. *Eur Arch Otorhinolaryngol*, 2022, 279(9): 4407-4414. doi: 10.1007/s00405-022-07271-4.
- [34] Rodrigues CT, Jacobs R, Vasconcelos KF, et al. Influence of CBCT-based volumetric distortion and beam hardening artefacts on the assessment of root canal filling quality in isthmus-containing molars[J]. *Dentomaxillofac Radiol*, 2021, 50(5): 20200503. doi: 10.1259/dmfr.20200503.

(编辑 张琳)



Open Access

This article is licensed under a Creative Commons Attribution 4.0 International License.
Copyright © 2024 by Editorial Department of Journal of Prevention and Treatment for Stomatological Diseases



官网